Comparing 3-Dimensional Virtual Methods for Reconstruction in Craniomaxillofacial Surgery

Stefano Benazzi, PhD, and Sascha Senck, MSc†*

Purpose: In the present project, the virtual reconstruction of digital osteomized zygomatic bones was simulated using different methods.

Materials and Methods: A total of 15 skulls were scanned using computed tomography, and a virtual osteotomy of the left zygomatic bone was performed. Next, virtual reconstructions of the missing part using mirror imaging (with and without best fit registration) and thin plate spline interpolation functions were compared with the original left zygomatic bone.

Results: In general, reconstructions using thin plate spline warping showed better results than the mirroring approaches. Nevertheless, when dealing with skulls characterized by a low degree of asymmetry, mirror imaging and subsequent registration can be considered a valid and easy solution for zygomatic bone reconstruction.

Conclusions: The mirroring tool is one of the possible alternatives in reconstruction, but it might not always be the optimal solution (ie, when the hemifaces are asymmetrical). In the present pilot study, we have verified that best fit registration of the mirrored unaffected hemiface and thin plate spline warping achieved better results in terms of fitting accuracy, overcoming the evident limits of the mirroring approach.

J Oral Maxillofac Surg 69:1184-1194, 2011

The introduction of computer-assisted preoperative planning and computer-assisted surgery has improved the outcome of craniomaxillofacial surgical intervention in recent years.[1] Advances in imaging techniques and the aid of computer-aided design (CAD)/computer-aided manufacturing (CAM) software provides the surgeon with an opportunity to perform virtual manipulations of computed tomography (CT) data preoperatively,[2] to simulate the entire surgical procedure in the computer, and to fabricate a physical model of the planned outcome.[3-5]

Preoperative planning is therefore crucial both to understand the problem to be solved and to find the best solution using less-invasive procedures.[6] Recently, several preoperative planning procedures have been proposed, and different applications were created for improved application and simplification. Some software provides facilities to perform translations of 3-dimensional (3D) objects in a virtual space, useful in the repositioning of displaced craniofacial elements. Pham et al[2] developed a technique for back conversion of surface or volume data to Digital Imaging and Communications in Medicine format using the Mimics software (Materialise, Leuven, Belgium). Surgeons were able to perform complex virtual reconstructions with the Mimics software and then converted the data to Digital Imaging and Communications in Medicine for use in any surgical navigation device. Mischkowski et al[7] developed software for the visual tracking of real anatomic structures in superimposition with 3D-rendered CT or magnetic resonance imaging scans for navigated translocation of bony segments. Furthermore, some surgeons prefer to simulate surgery on physical models produced by rapid prototyping techniques, usually stereolithography, onto which it is possible to customize implants or to precontour fixation plates. This information can be directly transferred to the patient by point-to-point computer-assisted navigation (eg, using the position of screws

Received from the Department of Anthropology, University of Vienna, Vienna, Austria.

*Researcher.

†PhD Student.

This work was supported by the EU Marie Curie Training Network (MRTN-CT-2005-019564 EVAN).

Address correspondence and reprint requests to Dr Benazzi: Department of Anthropology, University of Vienna, Althanstraße 14, Vienna 1090, Austria; e-mail: stefano.benazzi@univie.ac.at

0278-2391/11/6904-0044$36.00/0
doi:10.1016/j.joms.2010.02.028

previously defined).[8] Nevertheless, other researchers have noted the limitations of this approach, including a bias in model reshaping according to the artistic aptitude of the technician and its reductive utility in certain complex situations.[3]

Independent of the approach, the aim of operation planning in oral and maxillofacial surgery is an optimization of the surgical result to restore function, form, and the esthetic appearance,[1,6,9,10] which is to a certain degree connected to the correction of facial asymmetry. To restore facial symmetry, a standard procedure for preoperative planning is performed using the mirroring tool for unilateral defects, reconstructing the asymmetric portion, with its normal counterpart working as the reference.[1,3,4,9,11] Nevertheless, Metzger et al,[12] after comparing the preoperative planning by mirroring of the unaffected side to the affected side with the surgical outcome, verified that the accuracy of this approach could be influenced by the natural asymmetry of the skulls. They demonstrated that repositioning of the zygomatic bone remains a challenge despite computer-assisted surgery procedures. Even if some inaccuracy in surgical reconstruction could be masked by the natural asymmetry of the face, the investigators suggested that for large defects other planning tools (eg, dynamic 3D deformation) should be used.

It has been well recognized that asymmetry characterizes human paired and unpaired skeletal segments.[13-15] In regard to the skull, in particular, facial bones, the more asymmetric the shape, the less reliable is the definition of the mid-sagittal plane, which is essential for mirroring procedures. Accordingly, mirroring the unaffected side in more or less symmetric skulls/faces could be a proper solution for bone reconstruction, but for more asymmetric skulls/faces, other solutions would be required.

The techniques for bone reconstruction using geometric morphometric methods that were developed in anthropology and paleoanthropology could provide valuable aid for "form and functional restoration" in the surgical field. Using this virtual approach to reconstruction, problems related to asymmetry, deformation,[16] and missing data could be solved,[17-20] at the same time reducing the subjective choices of the operator and increasing the reliability and reproducibility of the result.[21]

In the present study, virtual osteotomy of the left zygomatic bone on 15 CT scans of human skulls stored in a database was performed. The outcomes of 3 virtual reconstruction techniques were compared with the original removed bone: *1*) mirroring of the unaffected hemiface; *2*) mirroring and subsequent registration of the unaffected hemiface onto the affected side; and *3*) thin plate spline (TPS) warping of the mirrored unaffected hemiface onto the affected side.

Materials and Methods

A total of 15 skulls were selected to simulate a virtual osteotomy (Table 1). Skulls 1 to 9 were dried skulls of modern Homo sapiens belonging to the collection of the Department of Anthropology and Anatomy, University of Vienna (Vienna, Austria). The CT scans were performed at the Radiologie 2 Medizinische Universität Innsbruck (Innsbruck, Austria), using a Siemens Somatom plus 40 scanner, with a slice thickness of 1 mm. Skulls 10 to 13 were dried skulls of modern Homo sapiens belonging to the collection at the Department of Paleobiology, Museo Nacional de Ciencas Naturales, Madrid, Spain. The CT scans were performed at the Ruber Clinic (Madrid, Spain), using a GE LightSpeed 16 scanner (GE Healthcare, Middle-

Table 1. LIST OF SKULLS

Label	Gender	Age (yr)	Origin	CT System
H1	Female	25	Europe	Siemens Somatom Plus 40
H2	Male	25	Europe	Siemens Somatom Plus 40
H3	Male	20	Europe	Siemens Somatom Plus 40
H4	Female	20	Australia	Siemens Somatom Plus 40
H5	Male	45	Australia	Siemens Somatom Plus 40
H6	Female	20	Africa	Siemens Somatom Plus 40
H7	Male	35	Asia	Siemens Somatom Plus 40
H8	Male	35	Asia	Siemens Somatom Plus 40
H9	Female	23	Europe	Siemens Somatom Plus 40
H10	Male	47	Europe	GE Light Speed 16
H11	Male	23	Europe	GE Light Speed 16
H12	Female	30	Europe	GE Light Speed 16
H13	Female	43	Europe	GE Light Speed 16
H14	Male	31	Europe	Brilliance CT 64-Slice by Philips
H15	Male	18	Europe	Brilliance CT 40-Slice by Philips

Benazzi and Senck. 3D Virtual Methods for Craniomaxillofacial Reconstruction. J Oral Maxillofac Surg 2011.

sex, United Kingdom), with a slice thickness of 0.625 mm. Skull H14 was from the Laboratory of Anthropology, Department of Histories and Method for the Conservation of Cultural Heritage (University of Bologna, Bologna, Spain). The CT scan was performed at the Radiology Department, Ravenna Hospital (Ravenna, Italy), using the Brilliance CT 64-slice scanner (Phillips Medical Systems, Eindhoven, The Netherlands), with a slice thickness of 0.9 mm and increment of 0.45 mm. Skull H15 (Fig 1) underwent CT scanning at the Pellegrin Hospital, Bordeaux, France, using the Brilliance CT 40-slice scanner, with a slice thickness of 0.9 mm and increment of 0.45 mm. The gender and age distribution for the skulls is listed in Table 1.

Digital models of the craniums were constructed semiautomatically using threshold-based segmentation, contour extraction, and surface reconstruction in Amira, version 5.2, software (Mercury Computer Systems, Chelmsford, MA) and saved as an "*.stl" model (Fig 1). Lower jaws were excluded because they were not required during the simulation. In Rapidform XOR (INUS Technology, Seoul, South Korea), left zygomatic virtual osteotomy was simulated in the digital models (Fig 2). This was accomplished by establishing 3 virtual cutting planes passing approximately through the following sutures: zygomomaxillary suture, frontozygomatc suture, and temporal-zygomatic suture on the zygomatic arc.

FIGURE 1. Skull H15. Representation of 3D surface model of cranium; left zygomatic portion in *dark gray*.

Benazzi and Senck. 3D Virtual Methods for Craniomaxillofacial Reconstruction. J Oral Maxillofac Surg 2011.

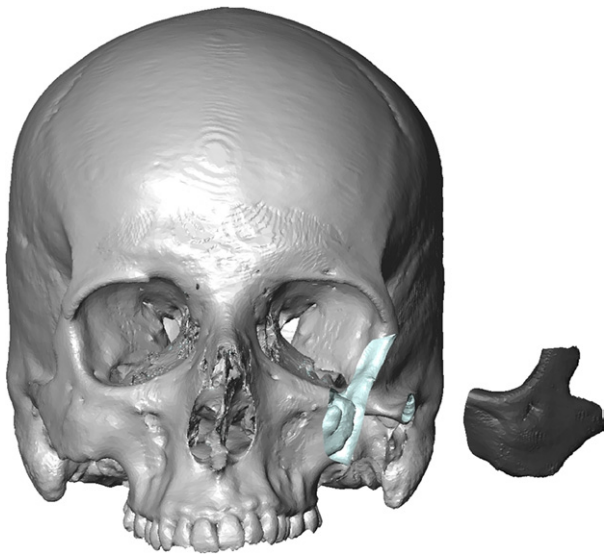

FIGURE 2. Skull H15. Virtual osteotomy of left zygomatic bone.

Benazzi and Senck. 3D Virtual Methods for Craniomaxillofacial Reconstruction. J Oral Maxillofac Surg 2011.

The mid-sagittal plane was defined as the best fit plane of 8 anatomic landmarks (prosthion, subspinale, nasion, bregma, lambda, inion, opisthion, staphylion). Three virtual reconstruction techniques were tested, computing the surface deviation of the reconstruction to the original skulls.

First, the right unaffected hemiface was mirrored, and the left missing part was directly restored using the mirrored copy without attempting any manual or automatic alignment of the reflected part onto the left hemiface.

Second, in Rapidform XOR, the right mirrored hemiface was aligned to the left osteomized hemiface using the iterative closest point, an algorithm that minimizes the distance between 2 point clouds by the least squares method.[22,23] Accordingly, the missing left part was replaced by the bone segment of the aligned right mirrored hemiface.

Finally, the mirrored cranium was warped onto the original one by applying the TPS algorithm.[17,18] The basic idea of TPS in missing data estimation is the warping of a complete reference configuration (reference model or template) onto an incomplete target (target model) based on homologous landmarks present in both the models, minimizing the thin plane spline's bending energy between the reference and the target.[24] Nevertheless, owing to the restricted amount of the anatomic landmarks in the maxillofacial region in our template, which could be further reduced after osteotomy, it was necessary to include semi-landmarks.[18] In detail, a template including 16 anatomic landmarks and 187 semi-landmarks was defined on the mirrored copy of the 15 skulls in

Edgewarp3D.[25] Another software program that could accomplish this procedure is Viewbox software (dHAL Software, Kifissia, Greece). Curves were digitized along the margin of the left orbit, the upper margin of the right orbit, from the stephanion to the frontotemporale, from the frontotemporale to the auriculare, on the lower margin of the zygomatic arc, and on the alveolar process, resulting in a total of 73 curve semi-landmarks (Figs 3, 4, and Table 2). Additionally, 114 surface semi-landmarks were digitized on the template (represented by the unaffected original skull).

Accordingly, a corresponding set of landmarks and curve semi-landmarks was created on the target models (the original resected craniums). After manual digitization of the 16 anatomic landmarks and 8 curves, the 73 curve semi-landmarks of the reference were automatically projected onto the respective curves digitized on the target models. Together with the anatomic landmarks, the curve semi-landmarks drove the TPS warping while guiding the 114 surface semi-landmarks closer to their position on the surface of the model.

Semi-landmarks that corresponded to the missing area were assigned 3 degrees of freedom (translation in x, y, and z direction), so that they were not forced to be projected and slid on the curves or the surface of the model. During the final sliding process, the geometric homology for the semi-landmarks on the curves and the surface was achieved between the reference template and the target. This step involved relaxing the curve semi-landmarks (sliding along tangent vectors to the curve and projection on the curve) and surface semi-landmarks (sliding along tangent planes to the surface and projection on the surface) of the target against the reference until the bending energy of the resulting TPS transformation was minimized.[18,26] It is worthwhile to emphasize that semi-landmarks with 3 degrees of freedom (related to the missing part) were involved in the sliding process but were not projected. The final outcome was a slid set of semi-landmarks for the target model, geometrically homologous to the semi-landmarks of the reference template (mirrored cranium).

The 203 landmarks and semi-landmarks of the reference and the target were imported into Amira, version 5.2. Using the "LandmarkSurfaceWarp" module; the surface of the reference was warped onto the specimen with the missing zygoma according to the landmarks and semi-landmarks of the template, using the Bookstein transformation mode according to the TPS interpolation.[26] This mode guarantees that the reference surface will be transformed exactly to the corresponding landmarks of

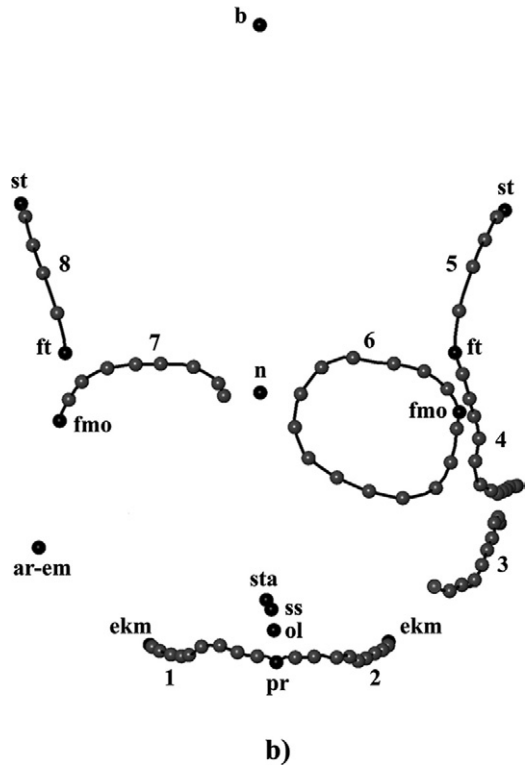

FIGURE 4. Skull H15. Landmarks and curves' semi-landmarks of template; landmarks and curve names listed in Table 2.

Benazzi and Senck. 3D Virtual Methods for Craniomaxillofacial Reconstruction. J Oral Maxillofac Surg 2011.

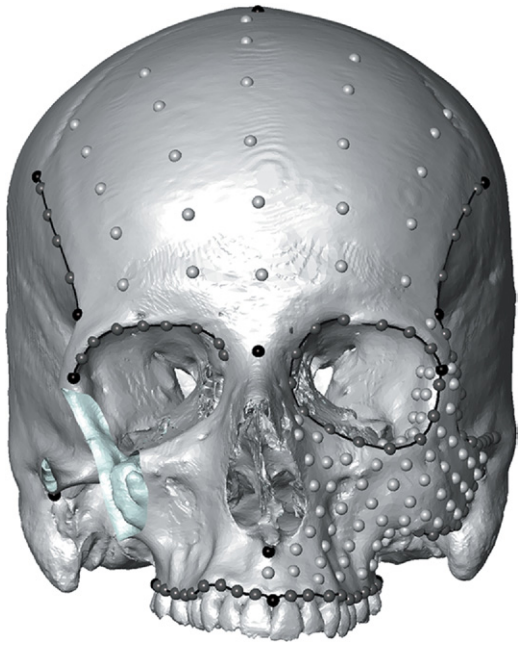

FIGURE 3. Skull H15. *A*, Set of landmarks and curves' semi-landmarks defined on reference model (template). *B*, landmarks and curves of semi-landmarks of template; landmarks and curve names are listed in Table 2.

Benazzi and Senck. 3D Virtual Methods for Craniomaxillofacial Reconstruction. J Oral Maxillofac Surg 2011.

Table 2. LIST OF LANDMARKS AND CURVES IDENTIFIED ON TEMPLATE

No.	Landmark Names	No.	Curve Names	Semi-Landmarks Indentified on Curves Count
1	Articulator eminence (ar-em) left	1	Alveolar right	9
2	Articulator eminence (ar-em) right	2	Alveolar left	9
3	Bregma (b)	3	Lower zygomaticotemporal outline left	10
4	Ektomolare (ekm) left	4	Upper zygomaticotemporal outline left	15
5	Ektomolare (ekm) right	5	Temporal left	4
6	Frontotemporale (ft) left	6	Orbital left	14
7	Frontotemporale (ft) right	7	Orbital right	8
8	Frontomalare orbitale (fmo) left	8	Temporal right	4
9	Frontomalare orbitale (fmo) right		Total semi-landmarks on curves	73
10	Nasion (n)			
11	Orale (ol)			
12	Prosthion (pr)			
13	Staphylion (stat)			
14	Stephanion (st) left			
15	Stephanion (st) right			
16	Subspinale (ss)			

Benazzi and Senck. 3D Virtual Methods for Craniomaxillofacial Reconstruction. J Oral Maxillofac Surg 2011.

the target, applying nearest neighbor interpolation for creating the final model.

The digital models obtained by TPS warping in Amira, version 5.2, were imported in Rapidform XOR, and the zygomatic segments were isolated using the cutting planes previously created for virtual zygomatic osteotomy.

To visualize and quantify the differences between the reconstructed zygomatic surface and the original osteotomized bone segments, deviation surface analyses were performed in Rapidform XOV/Verifier (INUS Technology). The original models were considered the reference surface. Using the "Auto Color Bar" function, the mean and standard deviation (SD) were automatically computed and color scales ranging from the minimum to maximum were created automatically displaying a signed color code onto the model's surface. The negative and positive values emphasized, respectively, the backward and forward displacement of the reconstruction compared with the original left zygomatic bone. For each reconstruction, the mean and SD were used for the Mann-Whitney *U* test to verify whether the reconstructions were significantly different from each other.

To quantify the total asymmetry of each individual face (object symmetry), we applied the Procrustes asymmetry assessment method from Mardia et al.[27] Starting from a facial landmark configuration of 3D coordinates (Table 3), total asymmetry was defined as the Procrustes distance between the original configuration (8 unpaired and 40 paired landmarks) and its relabeled reflection.[28-30]

The computation of total asymmetry for each skull incorporated the following steps: *1*) for each individual landmark configuration of the facial bone, a mirrored and appropriately relabeled form is produced;

Table 3. LIST OF LANDMARKS USED TO QUANTIFY TOTAL ASYMMETRY OF EACH INDIVIDUAL FACE

Unpaired Landmarks		Paired Landmarks			
No.	Landmark Names	No.	Landmark Names	No.	Landmark Names
1	Glabella	9	Frontotemporale	19	M^1-P^{2*}
2	Nasion	10	Frontomalare temporale	20	P^2-P^{1*}
3	Rhinion	11	Frontomalare orbitale	21	P^1-C^*
4	Subspinale	12	Jugale	22	$C-I^{2*}$
5	Prosthion	13	Zygomaxillare	23	I^2-I^{1*}
6	Orale	14	Zygo-orbitale	24	Zygotemporale superior
7	Incisivion	15	Apertura piriformes	25	Zygotemporale inferior
8	Staphylion	16	Foramen infraorbitale	26	Foramen palatinum anterior
		17	M^3-M^{2*}	27	Sutura sphenozygomatica
		18	M^2-M^{1*}	28	Maxilla distal

*Landmark digitized in alveolar process between 2 maxillary teeth.

Benazzi and Senck. 3D Virtual Methods for Craniomaxillofacial Reconstruction. J Oral Maxillofac Surg 2011.

2) each individual and its mirror was projected into the shape space using a generalized Procrustes analysis.[26,31] This involves translating, rescaling, and rotating the landmark configurations relative to each other to minimize the overall sum of squared distances between corresponding landmarks. The rescaling adjusts the landmark coordinates so that each configuration has a unit centroid size (square root of the summed squared Euclidean distances from all semi-landmarks to their centroid).[32] *3*) The total asymmetry was defined as the Procrustes distance (the square root of the sum of squared differences between the coordinates of the corresponding landmarks) between the original landmark configuration and its relabeled reflection.[28] Because after generalized Procrustes analysis, each individual is in shape space, the Procrustes distance between each individual and its mirror is rather small. It does not necessarily describe a biologic process but provides general information about facial asymmetry, but the exact location of asymmetry is omitted. In the present study, the Procrustes distance between each individual and its mirror was merely accounted as additional information that could help to interpret the outcome of the reconstruction. For data processing and analyses, we used software routines written in R software.[33]

Finally, as an example, a more detailed description of the outcome obtained in 2 cases with different values of total asymmetry (skulls H14 and H15) is provided.

Results

The mean and SD between the reconstructed surfaces and the original surface of the 15 resected zygomatic bones are listed in Table 4. Small mean values and the attendant reduced SDs established the criteria for the success of correct reconstructions.

The mirror method had larger mean and SD values than the other methods (Table 4), even if the difference in the mean values between the paired groups was not statistically significant ($P > .05$). The SD obtained for method 1 differed significantly from that for method 2 ($P < .0037$) or method 3 ($P < .0001$). When the comparison was between methods 2 and 3, the results were not significant, even if near to the statistically significant level ($P = .075$).

The individual facial asymmetry (Table 4) is related to the entire face and could mask the real amount of asymmetry present in the specific facial bone. Nevertheless, our results suggest that high individual asymmetry values (such as those obtained for skulls H2 and H15) should induce larger mean or SD values in the reconstruction using the mirroring tool.

FIRST EXAMPLE: SKULL H14

Skull H14 was characterized by low total facial asymmetry (Table 4). By mirroring the unaffected side without attempting any additional correction of the mirrored model position, the deviation between the original and mirrored surface was +1 to −1.5 mm (Figs 5, 6). In the frontal and temporal process of the zygomatic bone, the reconstructed model was posi-

Table 4. INDIVIDUAL ASYMMETRY,* MEAN,† AND STANDARD DEVIATION OF RECONSTRUCTIONS COMPARED WITH ORIGINAL LEFT ZYGOMATIC BONE‡

		Mirror		Mirror Registered		TPS Warping	
List of Skulls	Total Asymmetry	Mean	SD	Mean	SD	Mean	SD
H1	0.00432	−0.497	0.903	−0.032	0.482	−0.142	0.453
H2	0.00837	−0.557	1.411	0.101	0.902	−0.385	0.429
H3	0.00482	0.317	1.105	0.166	0.535	−0.679	0.514
H4	0.00619	−0.249	1.204	−0.047	0.502	0.387	0.402
H5	0.00703	−0.847	1.282	−0.186	0.970	0.342	0.766
H6	0.00477	−0.453	1.425	−0.467	1.254	−0.108	0.714
H7	0.00464	−0.033	0.815	0.142	0.767	0.481	0.499
H8	0.00526	0.078	1.125	0.605	0.836	0.072	0.622
H9	0.00554	0.352	1.551	0.071	0.628	−0.254	0.781
H10	0.00613	1.308	0.478	0.179	0.465	−0.011	0.429
H11	0.00747	−0.861	0.918	−0.113	0.395	0.133	0.352
H12	0.00467	1.602	0.669	−0.268	0.633	0.034	0.387
H13	0.00515	−0.772	0.718	−0.089	0.361	−0.041	0.307
H14	0.00433	−0.352	0.843	−0.044	0.579	−0.280	0.746
H15	0.00746	−1.458	2.085	−0.715	0.993	−0.295	0.627

*Total asymmetry computed as Procrustes distance (original skull [i] − mirror individual [i]).
†Negative sign underlines that average deviation of reconstruction was backward displaced compared with original bone.
‡Measurements in millimeters.

Benazzi and Senck. 3D Virtual Methods for Craniomaxillofacial Reconstruction. J Oral Maxillofac Surg 2011.

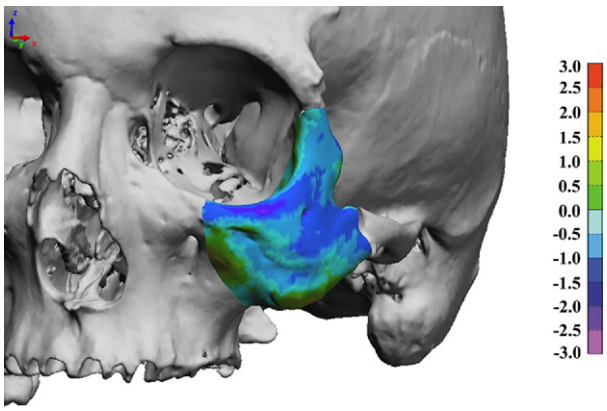

FIGURE 5. Skull H14, anterolateral view. Reconstruction using method 1. Color map illustrating distance between reconstruction and original model (in millimeters).

Benazzi and Senck. 3D Virtual Methods for Craniomaxillofacial Reconstruction. J Oral Maxillofac Surg 2011.

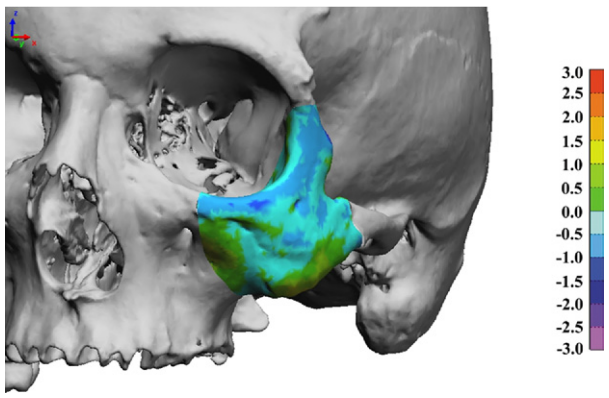

FIGURE 7. Skull H14, anterolateral view. Reconstruction using method 2.

Benazzi and Senck. 3D Virtual Methods for Craniomaxillofacial Reconstruction. J Oral Maxillofac Surg 2011.

tioned slightly backward compared with the original (−0.5/−1.0 to −1.0/−1.5 mm, respectively). Similar results were obtained for the anterior rim of the orbit (−1.0/−1.5 mm).

The deviation measured in the maxillary region and in the lower aspect of the zygomatic bone (−0.5/+1 mm) could have been related to the somewhat larger size of the mirrored model in those specific areas. This was supported by the results obtained from the second method, in which an alignment between the hemifaces was performed before isolating the zygomatic segment (Figs 7, 8). The maxillary and lower zygomatic region of the reconstructed model were slightly larger than the original.

Nevertheless, the overall result improved, and the mean and SD were clearly reduced (Table 4). Compared with the former reconstruction, the position of the reconstructed bone with regard to critical areas, such as the temporal process of the zygomatic bone, the lateral orbital wall, and the lower orbital rim, was noteworthy.

The results did not significantly differ when the reconstruction was performed using the TPS interpolation (Figs 9, 10, and Table 4). Nevertheless, the continuity between the reconstruction and the original bone near the resected areas was correctly reproduced.

SECOND EXAMPLE: SKULL H15

Unsatisfactory results were obtained using the mirroring tool for skull H15 (Figs 11, 12, and Table 4). This certainly resulted from the larger amount of total facial asymmetry (Table 4). Consequently, the frontal process of the zygomatic segment deviated more than 4 mm backward from the original bone, and the latero-orbital floor was more than 4 mm upward. A backward position of the virtual reconstruction is also displayed in the lower orbital rim and in the temporal process (Figs 11, 12).

The mean distances between the reconstruction and the original decreased when method 2 was used (Figs 13, 14, and Table 4). The surface deviation between the 2 compared models was reduced in both

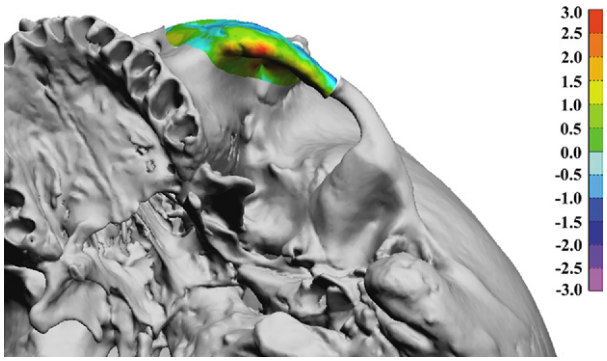

FIGURE 6. Skull H14, basal view. Reconstruction using method 1.

Benazzi and Senck. 3D Virtual Methods for Craniomaxillofacial Reconstruction. J Oral Maxillofac Surg 2011.

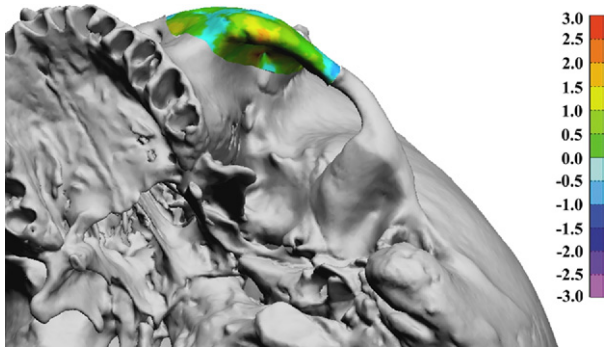

FIGURE 8. Skull H14, basal view. Reconstruction using method 2.

Benazzi and Senck. 3D Virtual Methods for Craniomaxillofacial Reconstruction. J Oral Maxillofac Surg 2011.

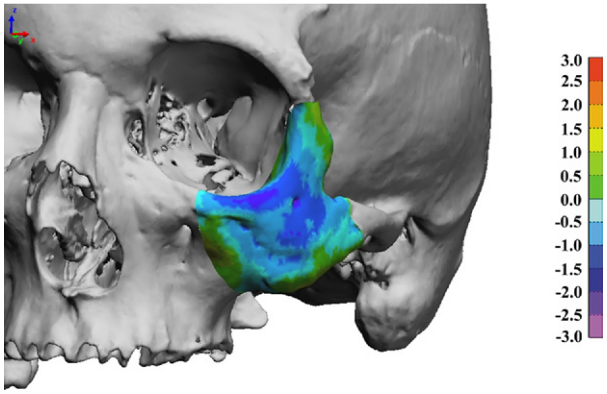

FIGURE 9. Skull H14, anterolateral view. Reconstruction using method 3.

Benazzi and Senck. 3D Virtual Methods for Craniomaxillofacial Reconstruction. J Oral Maxillofac Surg 2011.

the lateral orbital wall (less than −2 mm) and the temporal process (about −1 mm) of the zygomatic bone. Similarly, the deviation was decreased in the latero-orbital floor (less than +2.5 mm). Nevertheless, differences between the original bone and the reconstruction persisted, for example in the inferior margin of the zygomatic bone (Figs 13, 14).

The best outcome was clearly provided using method 3 (Figs 15, 16, and Table 4). The deviation was generally reduced by −0.5/+0.5 mm (about +1 mm in the latero-orbital floor), and a smooth continuity in the contact area between the reconstruction and the original cranium was achieved. This was one of the major contributions provided by the TPS-based reconstruction. For all 15 skulls (and hence not limited to skulls H14 and H15), the contact area between the reconstructed bone and the original bone was always more continuous than that provided by the mirror or mirror-registered tool.

Discussion

Function and esthetic restoration are the basic goals of craniomaxillofacial reconstruction.[1,9] As mentioned by some research that studied attractiveness[34,35] and regarding the general principle followed by surgeons, restoration of a symmetric shape could improve the outward appearance and hence provide a remarkable contribution to the quality of life. It is also obvious that functional restoration does not depend on this assumption, because it is possible to restore functionality without following strict symmetric intentions. Esthetics, in contrast, is somewhat associated with symmetry. We are aware that the human craniofacial anatomy is characterized by a certain degree of asymmetry (both skeletal and soft tissue). More precisely, the degree of interindividual variation is high. This concept is fundamental to reconstruction purposes.

In general, we have verified that the mirroring tool is not always the correct solution for zygomatic bone reconstruction, mainly when the individual face is highly asymmetric. More precise outcomes can be provided by either registration of the mirrored unaf-

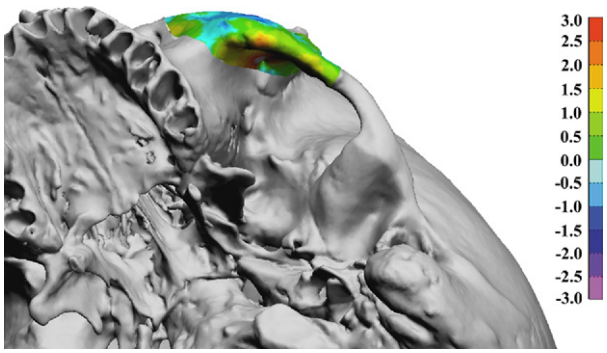

FIGURE 10. Skull H14, basal view. Reconstruction using method 3.

Benazzi and Senck. 3D Virtual Methods for Craniomaxillofacial Reconstruction. J Oral Maxillofac Surg 2011.

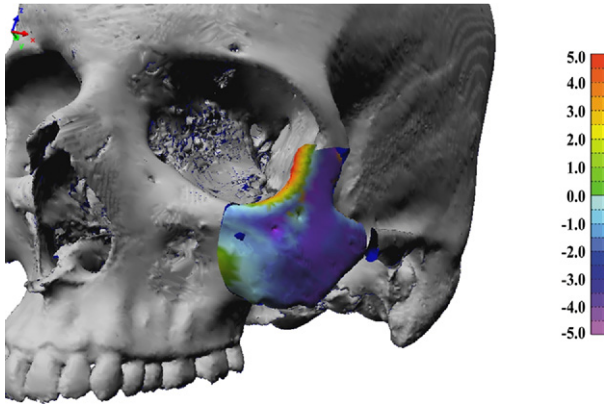

FIGURE 11. Skull H15, anterolateral view. Reconstruction using method 1. Color map illustrating distance between reconstruction and original model (in millimeters).

Benazzi and Senck. 3D Virtual Methods for Craniomaxillofacial Reconstruction. J Oral Maxillofac Surg 2011.

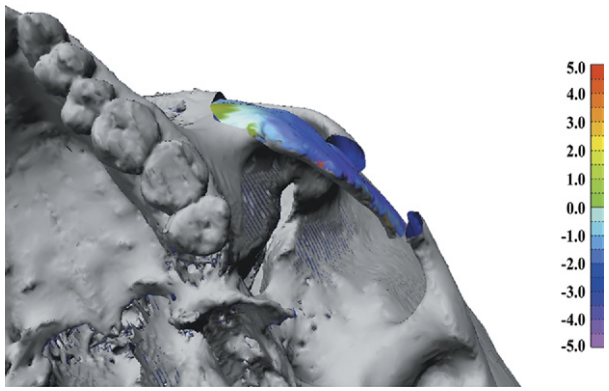

FIGURE 12. Skull H15, basal view. Reconstruction using method 1.

Benazzi and Senck. 3D Virtual Methods for Craniomaxillofacial Reconstruction. J Oral Maxillofac Surg 2011.

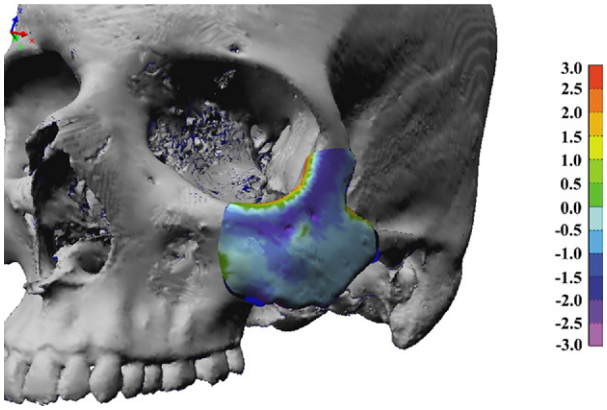

FIGURE 13. Skull H15, anterolateral view. Reconstruction using method 2.

Benazzi and Senck. 3D Virtual Methods for Craniomaxillofacial Reconstruction. J Oral Maxillofac Surg 2011.

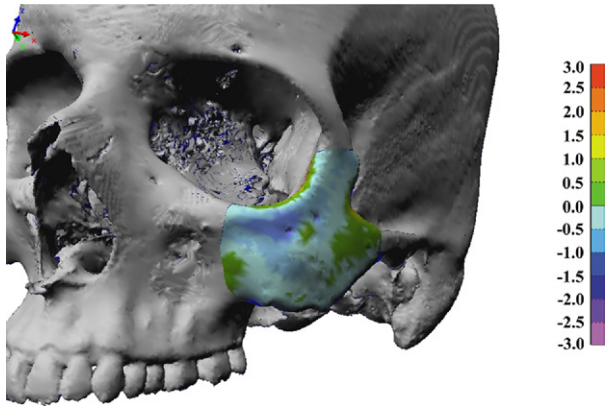

FIGURE 15. Skull H15, anterolateral view. Reconstruction using method 3.

Benazzi and Senck. 3D Virtual Methods for Craniomaxillofacial Reconstruction. J Oral Maxillofac Surg 2011.

fected hemiface on the affected hemiface or TPS warping of the mirrored cranium onto the original one. There is not one solution for bone reconstruction; thus, the more reliable outcome depends on the specific case under study. A preliminary computation of the total individual facial asymmetry (Table 4) could be a valid method to determine which approach could provide the best outcome. Even if the Procrustes distance between the landmark configuration of the original individual face and its reflection accounts for the entire facial asymmetry (which could somehow mask local asymmetric variation in specific bone portions), this value could provide a useful tool for selecting which reconstruction technique should be used in each situation. Accordingly, we emphasized the necessity to explore this interesting topic further.

Skull H14 is a typical example of low individual asymmetry, in which the unaffected hemiface could be directly used as a reference for replacing the defect of the affected side. However, as shown in Figures 7 and 8A, preliminary alignment between the 2 models was suggested before isolating the replacement segment.

In the second example (skull H15), the mirroring tool failed to provide a reliable solution for reconstruction. Even if the incorrect outcome of the mirroring procedure could be improved by performing alignment between the 2 models, the result was still unsatisfactory, particularly regarding the accuracy of fit of the involved temporal and frontal processes. To restore function and provide an esthetic appearance, a reliable alternative could be TPS warping. In all virtual simulations, models reconstructed by TPS displayed a small mean deviation and reduced SD with respect to the original osteotomized model and an adequate continuity with the original surrounding bone (Figs 15, 16).

The approach using TPS interpolation functions was among those used in paleoanthropology for fossil

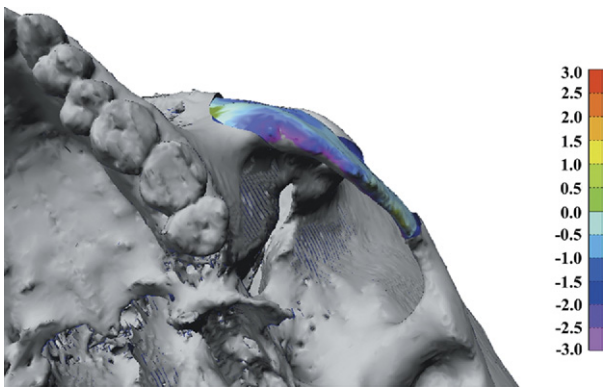

FIGURE 14. Skull H15, basal view. Reconstruction using method 2.

Benazzi and Senck. 3D Virtual Methods for Craniomaxillofacial Reconstruction. J Oral Maxillofac Surg 2011.

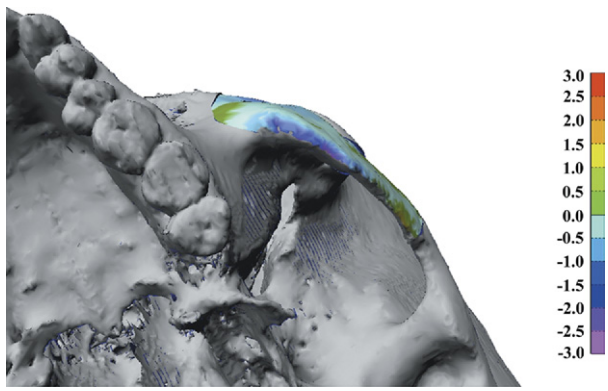

FIGURE 16. Skull H15, basal view. Reconstruction using method 3.

Benazzi and Senck. 3D Virtual Methods for Craniomaxillofacial Reconstruction. J Oral Maxillofac Surg 2011.

reconstruction[18] and in forensic anthropology for the reconstruction of a fragmented skull.[19] It was recently used in physical anthropology for the virtual reconstruction of missing condyles.[20] Unlike the mirroring procedure, TPS tries to warp the reference shape to the target shape using a set of corresponding landmarks or semi-landmarks. Because symmetry between hemifaces is not relevant, the reconstructed model will be somewhat asymmetric compared with the reference. The outcome will depend on both the morphometric features of the target shape and the size of the area to be reconstructed. Although the former is obvious (the more asymmetric the target shape, the more asymmetric the reconstruction), the latter point requires additional explanation. As mentioned, thin plate splines are used to establish geometric homology between 2 sets of semi-landmarks (reference and target) to estimate the position of the missing landmarks. The TPS functions bend the spline near existing landmarks, and the estimation of the missing data was best in the proximity of the preserved part in which the landmarks are supposed to be placed. Increasing the size of the osteotomy will reduce the probability of finding anatomic landmarks useful to bend the spline in the vicinity of the missing data; then the TPS grid will be almost square.[18] Thus, the further the location of the estimated landmarks from the preserved surface, the closer they will resemble the reference shape.

In the virtual reconstruction of the zygomatic segment, the area surrounding the osteotomy was marked by several landmarks and semi-landmarks according to which the TPS function bends the spline, allowing an estimation of the missing data. Accordingly, regarding the amount of surface deviation between the reconstruction and the original zygomatic bone (Table 4), TPS is able to establish continuity between the reconstructed and original bone near the resected area. The approach using TPS warping is more time-consuming than the mirror-registered method, and the usefulness of the method requires a careful evaluation of the specific problem.

Finally, it is also worthwhile to emphasize that the method could be useful if the defect is not limited to one hemiface but involves more or less extensively both hemifaces. As reported by Benazzi et al,[19] an external reference shape, morphometrically similar to the face to be reconstructed, can be warped to the target shape. To deal with this scenario, a "virtual skull database" useful for selecting the best reference shape should be available. It is evident that the same limitations will persist: the fewer landmarks present to bend the spline near the missing data, the more the reconstruction will be similar to the reference shape.

Using computer-assisted preoperative planning for surgical simulation, surgeons have the possibility of testing different reconstruction approaches in 3D virtual space that allows precise visualization of the simulated outcome. The mirroring procedure is one of the possible alternatives useful in reconstruction but might not always be the optimal solution (ie, when the hemifaces are considerably asymmetric). In the present pilot study, the mirror-registered approach and the TPS technique achieved better results, overcoming the primary limits of the mirroring approach.

To date, the TPS technique has been used for reconstruction in anthropology and paleoanthropology, in which the limits of the mirroring approach are well known. Therefore, it is important to emphasize that the TPS technique has the potential to become a valuable tool in craniomaxillofacial surgery, providing improvement in the accuracy of bone reconstruction.

Acknowledgment

We wish to express our gratitude and thanks to Dr Demetrios Halazonetis for his help and valuable advice. We are also grateful to Stephanie Kozakowski for copy editing the manuscript. We thank Antonio Rosas González (Museo Nacional de Ciencias Naturales, Madrid, Spain) and G.W. Weber (Department of Anthropology, University of Vienna, Vienna, Austria) for access to CT data by way of NESPOS (Neanderthal Studies Professional On-line Service) and EVAN (European Virtual Anthropology Network).

References

1. Kokemueller H, Tavassol F, Ruecker M, et al: A combined technique of computer-assisted surgery and microvascular tissue transfer. J Oral Maxillofac Surg 66:2398, 2008
2. Pham AM, Rafii AA, Metzger MC, et al: Computer modeling and intraoperative navigation in maxillofacial surgery. Otolaryngol Head Neck Surg 137:624, 2007
3. Wong TY, Fang JJ, Chung CH, et al: Comparison of 2 methods of making surgical models for correction of facial asymmetry. J Oral Maxillofac Surg 63:200, 2005
4. Gateno J, Xia JJ, Teichgraeber JF, et al: Clinical feasibility of computer-aided surgical simulation (CASS) in the treatment of complex cranio-maxillofacial deformities. J Oral Maxillofac Surg 65:728, 2007
5. Xia JJ, Gateno J, Teichgraeber JF, et al: Accuracy of the computer-aided surgical simulation (CASS) system in the treatment of patients with complex craniomaxillofacial deformity: A pilot study. J Oral Maxillofac Surg 65:248, 2007
6. Hassfeld S, Mühling J: Computer assisted oral and maxillofacial surgery—A review and an assessment of technology. Int J Oral Maxillofac Surg 30:2, 2001
7. Mischkowski RA, Zinser MJ, Kübler AC, et al: Application of an augmented reality tool for maxillary positioning in orthognathic surgery—A feasibility study. J Craniomaxillofac Surg 34:478, 2006
8. Klug C, Schicho K, Ploder O, et al: Point-to-point computer-assisted navigation for precise transfer of planned zygoma osteotomies from the stereolithographic model into reality. J Oral Maxillofac Surg 64:550, 2006
9. Schmelzeisen R, Gellrich NC, Schoen R, et al: Navigation-aided reconstruction of medial orbital wall and floor contour in cranio-maxillofacial reconstruction. Inj Int J Care Injured 35: 955, 2004
10. Voss PJ, Leow AM, Schulze D, et al: Navigation-guided resection with immediate functional reconstruction for high-grade malignant parotid tumour at skull base. Int J Oral Maxillofac Surg 38:886, 2009

11. Hohlweg-Majert B, Schön R, Schmelzeisen R, et al: Navigational maxillofacial surgery using virtual models. World J Surg 29: 1530, 2005
12. Metzger MC, Hohlweg-Majert B, Schön R, et al: Verification of clinical precision after computer-aided reconstruction in craniomaxillofacial surgery. Oral Surg Oral Med Oral Pathol Oral Radiol Endod 104:e1, 2007
13. Auerbacha BM, Ruff CB: Limb bone bilateral asymmetry: Variability and commonality among modern humans. J Hum Evol 50:203, 2006
14. Gawlikowska A, Szczurowski J, Czerwiński F, et al: The fluctuating asymmetry of medieval and modern human skulls. Homo 58:159, 2007
15. Auerbacha BM, Raxter MH: Patterns of clavicular bilateral asymmetry in relation to the humerus: Variation among humans. J Hum Evol 54:663, 2008
16. Ogihara N, Nakatsukasa M, Nakano Y, et al: Computerized restoration of nonhomogeneous deformation of a fossil cranium based on bilateral symmetry. Am J Phys Anthropol 130:1, 2006
17. Gunz P, Mitteroecker P, Bookstein FL, et al: Computer aided reconstruction of incomplete human crania using statistical and geometrical estimation methods. Enter the Past: Computer Applications and Quantitative Methods in Archaeology, BAR International Series 1227. Oxford, Archaeopress, 2004, p 92-94
18. Gunz P, Mitteroecker P, Bookstein FL: Semilandmarks in three dimensions, *in* Slice DE (ed): Modern Morphometrics in Physical Anthropology. New York, Kluwer Academic/Plenum Publishing, 2005, pp 73-98
19. Benazzi S, Stansfield E, Milani C, et al: Geometric morphometric methods for three-dimensional virtual reconstruction of a fragmented cranium: The case of Angelo Poliziano. Int J Leg Med 123:333, 2009
20. Benazzi S, Stansfield E, Kullmer O, et al: Geometric morphometric methods for bone reconstruction: The mandibular condylar process of Pico della Mirandola. Anat Rec 292:1088, 2009
21. Weber G: Virtual anthropology (VA): A call for glasnost in paleoanthropology. Anat Rec 265:193, 2001
22. Besl PJ, McKay ND: A method for registration of 3-d shapes. PAMI 14:239, 1992
23. Zhang ZY: Iterative point matching for registration of free-form curves and surfaces. Int J Comput Vis 13:119, 1994
24. Gunz P, Mitteroecker P, Neubauer S, et al: Principles for the virtual reconstruction of hominin crania. J Hum Evol 57:48, 2009
25. Bookstein FL, Green WK: Edgewarp 3D, 2002. Available from: brainmap.stat.washington.edu/edgewarp/. Accessed April 8, 2010
26. Bookstein FL (ed): Morphometric Tools for Landmark Data: Geometry and Biology. New York, Cambridge University Press, 1997
27. Mardia KV, Bookstein F, Moreton I: Statistical assessment of bilateral symmetry of shapes. Biometika 87:285, 2000
28. Klingenberg CP, Barluenga M, Meyer A: Shape analysis of symmetric structures: Quantifying variation among individuals and asymmetry. Evolution 56:1909, 2002
29. Schaefer K, Lauc T, Mitteroecker P, et al: Dental arch asymmetry in an isolated Adriatic community. Am J Phys Anthropol 129:132, 2006
30. Mitteroecker P, Gunz P: Advances in geometric morphometrics. Evol Biol 36:235, 2009
31. Rohlf FJ, Slice DE: Extensions of the Procrustes method for the optimal superimposition of landmarks. Syst Zool 39:40, 1990
32. Dryden IL, Mardia KV: Statistical Shape Analysis. New York, John Wiley and Sons, 1998
33. R Development Core Team, *in* R: A Language and Environment for Statistical Computing: R. Vienna, Austria, Foundation for Statistical Computing, 2008. Available from: www.r-project.org. Accessed April 8, 2010
34. Penton-Voak IS, Jones BC, Little AC, et al: Symmetry, sexual dimorphism in facial proportions, and male facial attractiveness. Proc Biol Sci 268:1617, 2001
35. Little AC, Jones BC, Waitt C, et al: Symmetry is related to sexual dimorphism in faces: Data across culture and species. PLoS ONE 3:e2106, 2008